Novel Length Scales in Nanotube Devices

François Léonard and J. Tersoff
IBM Research Division, T. J. Watson Research Center, P.O. Box 218, Yorktown Heights, New York 10598
(Received 21 July 1999)

We calculate the properties of p-n junctions, n-i junctions, and Schottky barriers made on a single-wall carbon nanotube. In contrast to planar bulk junctions, the depletion width for nanotubes varies *exponentially* with inverse doping. In addition, there is a very long-range (*logarithmic*) tail in the charge distribution, extending over the entire tube. These effects can render traditional devices unworkable, while opening new possibilities for device design. Our general conclusions should apply to a broad class of nanotube heterojunctions, and to other quasi-one-dimensional "molecular wire" devices.

PACS numbers: 85.30.Vw, 73.40.Lq, 73.40.Ns, 73.61.Wp

The prospect of nanoscale electronic devices has excited great interest, with proposals ranging from quantum-dot cellular automata [1] to molecular switches [2]. Carbon nanotubes (NTs) hold particular promise—though only a nanometer across, they have exceptional strength and stability, and they can be either metallic or semiconducting [3]. Simple field-effect NT transistors have already been demonstrated [4,5]. Perhaps the most exciting possibility lies in devices fabricated on a single tube [6], which in principle permit extremely small size and high density.

Here we examine the simplest possible on-tube device, the p-n junction, as well as n-i junctions and metal-NT Schottky barriers. We find that NT devices differ dramatically from classic planar devices. In particular, the depletion length varies *exponentially* with inverse doping. At low doping the depletion length grows to microns or more, precluding a nanoscale device. At high doping, the length scale becomes so small that the device is essentially short-circuited by tunneling [7]. There is at most a narrow window between these two regimes. Thus any useful implementation would probably require new device designs, and we suggest a design for a NT rectifier.

In addition, charging is not confined to the depletion region, but extends over the entire tube, decaying only *logarithmically* with distance from the junction. Thus charge-transfer doping takes on radically greater importance in NT devices. This can pose serious problems, but it also provides new opportunities for device design.

The novel behavior here is largely due to the quasi-one-dimensional electrostatics and screening, and so should hold qualitatively for a broad range of NT devices, such as on-tube heterojunctions [6], and for quasi-one-dimensional "molecular wire" devices in general.

We treat a single-walled semiconducting NT of radius R and band gap E_g surrounded by a dielectric. To form a p-n junction, one half of the NT is uniformly n doped, while the other half has equal and opposite p doping. This is equivalent (via an image-potential construction) to a Schottky barrier formed by an n- or p-doped NT contacting a planar metal electrode, with a Schottky barrier height equal to half the NT band gap. For the n-i junction, half of the NT is uniformly n doped while the other half is undoped ("intrinsic"). Our general qualitative conclusions also apply to asymmetric p-n junctions or Schottky barriers.

Substitutional doping of NTs with B and N has been predicted theoretically [8], and substitution of B has been observed in C_{60} molecules [9]. Doping by insertion of alkali or halogen atoms inside the tube has also been proposed [10], and similar doping might be possible by binding appropriate atoms or molecules to the outside of the tube. It is not yet clear which is the most promising mechanism for doping, much less the precise donor and acceptor levels. We therefore adopt a generic model for the doping, where the extra charge is uniformly distributed over the tube so it does not affect the band structure. This model appears to be well justified for the case of doping by the insertion of atoms inside the tube [10].

The (screened) charge σ per atom along the tube is the sum of contributions from dopant ions and electrons. On the n-type side of the junction,

$$\sigma(z) = \frac{e}{\epsilon} f - \frac{e}{\epsilon} \int_{E_c(z)}^{\infty} D(E,z) F(E)\, dE + \sigma^{\mathrm{scr}}, \quad (1)$$

where f is the doping fraction (the number of dopants per atom of the NT), ϵ is the dielectric constant of the surrounding material, $D(E,z)$ is the local density of states per atom, $F(E)$ is the Fermi function, and $E_c(z)$ is the local conduction-band edge. We can neglect the valence-band contribution since the band gap $E_g \gg k_B T$.

The screening charge σ^{scr} includes the dielectric polarization of the NT itself. In addition, Eq. (1) implicitly assumes a space-filling dielectric, so σ^{scr} also contains a term to cancel the contribution of dielectric material where there is actually a hole to accommodate the NT. These two terms correspond to dielectric rods of similar radius, but contributing charges of opposite sign. Thus the two terms tend to cancel. Also, both become unimportant at large length scales. We therefore neglect σ^{scr} for simplicity.

The charge is calculated using the "universal" NT density of states [11], rigidly shifted by the local electrostatic

 0031-9007/99/83(24)/5174(4)$15.00

potential $V(z)$:

$$D(E,z) = \frac{a\sqrt{3}}{\pi^2 R V_0} \sum_{m=-\infty}^{m=\infty} g[E, \varepsilon_m - \mathrm{eV}(z)], \quad (2)$$

where $g(E,\varepsilon) = (1 - \varepsilon^2/E^2)^{-1/2}$ for $|E| > \varepsilon$, and zero otherwise. Here $\varepsilon_m = |3m - 1| a V_0/2R$, V_0 is the π-band tight-binding parameter, and a is the bond length. The accuracy of this approximation is discussed below.

The charge on the tube induces an electrostatic potential

$$V(z) = \frac{R}{4\pi} \int \sigma(z') G(z - z')\, dz', \quad (3)$$

where G is the electrostatic kernel for a cylinder. We obtain the band bending and charge distribution by self-consistently solving Eq. (1) (and the corresponding equation for the p type or undoped side of the junction) and Eq. (3). The computation is performed in Fourier space, for a periodic array of junctions. The parameters used in our calculations are those of typical semiconducting nanotubes at room temperature [12,13], embedded in SiO_2: $R = 0.7$ nm, $E_g = 0.6$ eV, $V_0 = 2.5$ eV, and $\epsilon = 3.9$.

Figure 1 shows the "band bending" at a NT p-n junction for doping fraction $f = 5 \times 10^{-4}$ and $f = 10^{-3}$. The charge density is shown in Fig. 2. While the band bending looks superficially similar to a classic planar device, the profound differences are seen immediately in the charge distribution. A planar bulk device has a region of essentially complete charge depletion, with an abrupt transition to an uncharged region [14]. In contrast, for NTs the region of complete depletion joins smoothly onto a tail, which decays extremely slowly. This tail is also present (though less conspicuous) in the band bending.

Qualitatively, the numerically calculated charge density has the form

$$\sigma(z) \sim \begin{cases} \sigma_0, & z < W, \\ \sigma_0 \ln(W/\lambda)/\ln(z/\lambda), & z > W, \end{cases} \quad (4)$$

where $\sigma_0 = ef/\epsilon$, and λ is a constant of order R independent of doping. This is shown explicitly in the inset of Fig. 2. Thus there are *two distinct length scales* that characterize the behavior: the width W of the region of full depletion, and the logarithmic-decay length $\lambda \sim R$ of the charge tail. Outside the region of full depletion, the charge decays extremely slowly—as $1/\ln(z/\lambda)$.

In a planar bulk junction, the charge in the depletion region creates a dipole sheet. The potential outside the sheet is constant, so there is no further band bending or charging outside this depletion region. For the NT p-n junction, the dipole sheet is replaced by a dipole ring. If charging were restricted to a finite depletion region, the potential would fall off as z^{-2} at large distances, which is inconsistent with having no charge at large distances. In fact, the potential must approach a constant value (the "bulk" charge-neutral value) at large distances, and it is this condition (in combination with the kernel G) which determines the asymptotic form of the charge.

The depletion width W is plotted as a function of doping in Fig. 3. Because $\sigma(z)$ is rounded by finite-temperature effects, there is some uncertainty in extracting W from our room-temperature numerical results. Two different criteria for W are used in Fig. 3: (1) the distance from the junction where the charge drops to 95% of σ_0, and (2) the distance from the junction where the potential comes within $2k_BT$ of the band edge or the asymptotic Fermi level. These give similar behavior.

For planar junctions, $W \sim f^{-1/2}$. The behavior of nanotubes is radically different, as seen in Fig. 3. For low doping we find that W depends exponentially on $1/f$, and can grow to microns or more. Moreover, in this case the charge tail decays extremely slowly. The charge drops by a factor of 2 at a distance $z = W^2/\lambda$, so this characteristic length for decay of the charge tail grows much faster even than W.

The exponential dependence of W on inverse doping can be rationalized by neglecting the charge outside of W.

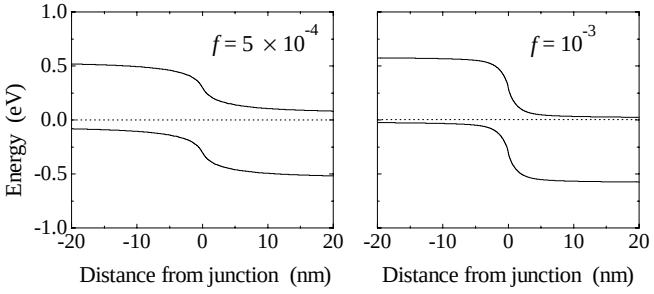

FIG. 1. Band diagram of nanotube p-n junction for doping $f = 5 \times 10^{-4}$ and 10^{-3}. Solid lines are local valence and conduction band edges. Dotted line is the Fermi level.

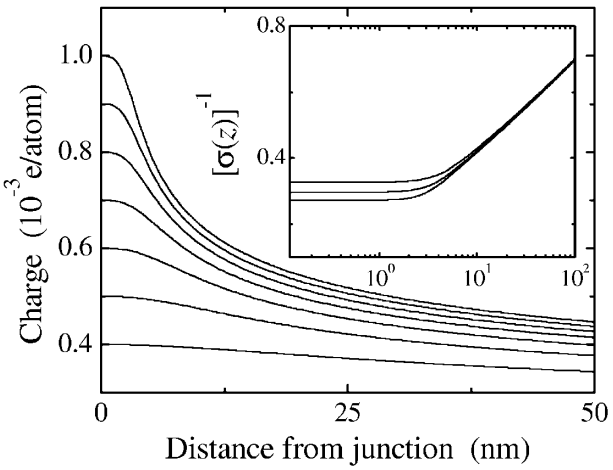

FIG. 2. Charge per C atom on the n-type side of the nanotube p-n junction. Curves from bottom to top are for doping fraction $f = 4 \times 10^{-4} - 10^{-3}$, in increments of 10^{-4}. Inset shows a scaling plot for $f = 8 \times 10^{-4}$, 9×10^{-4}, and 10^{-3}, normalized to 1 at 1 μm from the junction.

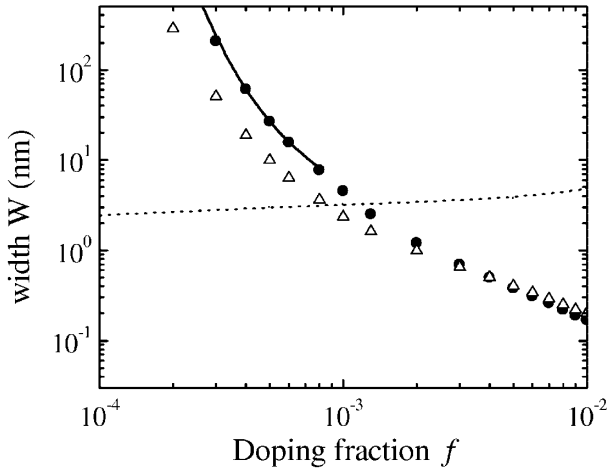

FIG. 3. Depletion width W vs doping fraction f, calculated two different ways (see text). Solid line is $Ae^{B/f}$, fitted to the low-f data. Dotted line is the rms width of the response function χ (see text).

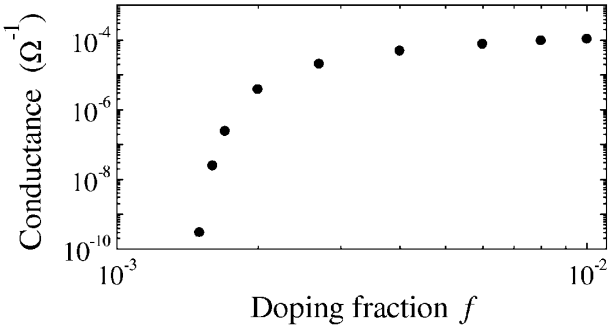

FIG. 4. Tunneling conductance at zero bias vs doping fraction f. See text for approximations.

Then, using the asymptotic form of $G(z)$ in Eq. (3), we obtain for $W \gg R$ the approximate expression $W \sim R \exp(\epsilon\epsilon_0 E_g/e^2 RNf)$, where ϵ_0 is the permittivity of free space. To the extent that the depletion width reflects the fixed ionic charge and the electrostatic kernel, it should be insensitive to the precise accuracy of Eq. (2).

At high doping, W is in the nanometer scale. In Eq. (2) we have approximated the free-carrier susceptibility $\chi(r - r') = d\sigma(r)/dV(r')$ as a strictly local function $\chi(r)\delta(r - r')$, so the actual width of $\chi(r - r')$ places a lower bound on the length scale at which our calculations are quantitatively accurate. We show the rms width of χ (within linear response theory and the effective-mass approximation) in Fig. 3 [15]. For $f > 10^{-3}$, the width of χ becomes greater than W, and our results are qualitative rather than quantitative. (For $f > 10^{-3}$, the average distance to the nearest dopant becomes comparable to W, so dopant fluctuations also become an interesting issue is this regime.) Since W already reaches the nanometer scale for $f \sim 10^{-3}$, our conclusions should be unaffected by the reduced accuracy at higher doping.

At low doping, the large depletion width presumably makes the device useless for nanoelectronics. The high-doping regime should be better for nanoscale applications, since the band bending and charge variation occur over nanoscale distances. Doping by alkali or halogen atoms packed inside nanotubes [10] corresponds to the extreme high-doping regime, $f \sim 10^{-2}$.

A potential limitation of the high-doping regime is the possibility of substantial tunneling currents across the junction. Such "leakage current" must be small for good device performance. We estimate the tunneling probability P for electrons at the Fermi level using the WKB approximation, $P = \exp[-2\int k_\parallel(z)\,dz]$, where the integral is between the classical turning points. Here $k_\parallel(z) = [2/(3aV_0)]\{(E_g/2)^2 - [\mathrm{eV}(z)]^2\}^{1/2}$ is the imaginary part of the wave vector.

The resulting conductance, $\Gamma = (4e^2/h)P$ (from the Landauer formula [16] with two channels), is shown in Fig. 4. (For a Schottky barrier, the electrons need only tunnel from the classical turning point to the metal electrode at the origin, so the conductance is larger than that shown in Fig. 4 but shows a similar variation with f.) For $f > 2 \times 10^{-3}$, the tunneling probability is of order 1, so the device gives poor rectification.

Below $f \sim 10^{-3}$, doping is nondegenerate at room temperature, so there are no states at the Fermi level for tunneling. Even in this regime, tunneling may be large at moderate reverse bias. Above $f \sim 10^{-3}$, the tunneling distance shrinks rapidly to around $2W$; at slightly higher doping, $4k_\parallel W$ is of order unity, giving substantial tunneling. This qualitative picture should remain true despite the limited accuracy of W and of the WKB approximation in this regime.

Thus, for the parameters used here, the p-n junction is rendered unsuitable as a nanoscale rectifier by tunneling for $f > 2 \times 10^{-3}$, and by the large depletion length for $f < 2 \times 10^{-4}$. This range depends somewhat on the values of tube radius R (which sets the band gap) and ϵ. Note that these constraints are only bounds, set by the depletion width and the low-voltage tunneling conductance. Consideration of the (much longer) length scale of the charge tail, and the increase in tunneling with reverse-bias voltage, may render the simple p-n junction unsuitable as a nanoscale rectifier at *any* f [7].

The long-range charge transfer may have important implications for other devices, and for doping in general. We illustrate this for an n-i junction, shown in Fig. 5. Because of the quasi-one-dimensional electrostatics, "charge-transfer doping" (analogous to modulation doping) is dramatically stronger than in planar devices. In planar junctions, charge transfer creates a quasi-two-dimensional electron gas confined near the interface. In contrast, for the NT there is significant charge transfer up to distances of microns or more. The carrier concentration one micron from the junction is 4 orders of magnitude

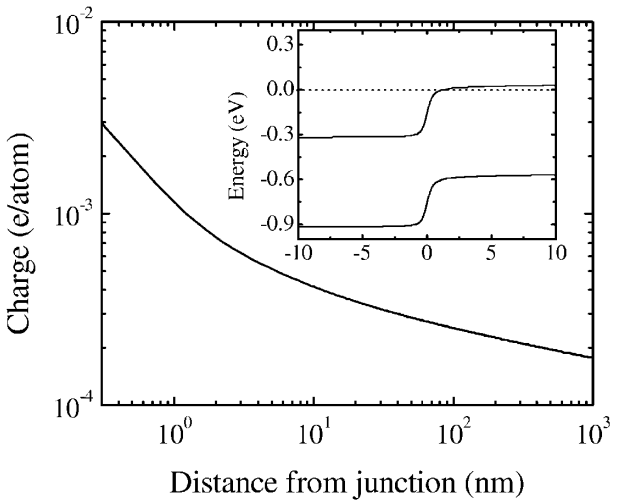

FIG. 5. Charge per C atom on the i side of the nanotube n-i junction. The n side is doped $f = 0.01$. Inset shows corresponding band diagram; dotted line is the Fermi level.

larger than in the isolated intrinsic tube, and corresponds to the same number of carriers per atom as a doping of 10^{18} cm^{-3} in bulk Si. This charge transfer drastically increases the conductivity of the intrinsic tube, and may permit new device designs for nanotubes, or provide a laboratory for fundamental studies of the one-dimensional electron gas without dopant scattering. In realistic device designs, the charge will depend on the electrostatic boundary conditions, providing further opportunities for control.

On the other hand, devices that require confinement of the carriers could no longer rely on the electrostatics of doping to provide strong confinement, and they might need to be redesigned. Also, there is evidence that NTs may be accidentally doped by atoms or molecules that attach during growth or processing [5], or by charge transfer from metal electrodes [4]. Because of the long range of any charge transfer, such accidental doping could severely affect performance unless taken into account in the design of NT devices.

The effects described here certainly do not preclude the successful operation of nanotube devices. For example, the leakage current due to tunneling in highly doped NT p-n junctions can be controlled by including a small undoped segment of length $L \gg W$ between the p- and n-doped regions. The band bending in this p-i-n system then occurs over the length L rather than W. We have verified this approach numerically. For $f = 10^{-2}$, the tunneling probability is reduced by a factor $\sim \exp(-2kL)$, where k is the imaginary part of the wave vector deep in the band gap. For $L = 15$ nm, the tunneling current is reduced by a factor $\sim 10^6$.

The essential point is that nanotube devices are not simply miniature versions of traditional devices. Because of their reduced dimensionality the electrostatics, doping, and charge transfer are dramatically different. Any attempt to design NT devices must take this novel behavior into account. While some traditional devices may become unworkable, there will doubtless be opportunities for other, entirely new device designs.

We are grateful to Phaedon Avouris and David Vanderbilt for stimulating discussions. F. L. acknowledges support from the NSERC of Canada.

[1] A. O. Orlov, I. Amlani, G. H. Bernstein, C. S. Lent, and G. L. Snider, Science **277**, 928 (1997).
[2] Y. Wada, Microelectron. Eng. **30**, 375 (1996).
[3] R. Saito, M. Fujita, G. Dresselhaus, and M. S. Dresselhaus, Appl. Phys. Lett. **60**, 2204 (1992).
[4] S. J. Tans, A. R. M. Verschueren, and C. Dekker, Nature (London) **393**, 49 (1998).
[5] R. Martel, T. Schmidt, H. R. Shea, T. Hertel, and Ph. Avouris, Appl. Phys. Lett. **73**, 2447 (1998).
[6] L. Chico, V. H. Crespi, L. X. Benedict, S. G. Louie, and M. L. Cohen, Phys. Rev. Lett. **76**, 971 (1996).
[7] A recent Letter predicted good rectification in a NT p-n junction: A. A. Farajian, K. Esfarjani, and Y. Kawazoe, Phys. Rev. Lett. **82**, 5084 (1999). That work used a strictly local model for the electrostatic interaction (the Hubbard model), which seems sufficient to account for the very different results.
[8] J.-Y. Yi and J. Bernholc, Phys. Rev. B **47**, 1708 (1993).
[9] T. Guo, C. Jin, and R. E. Smalley, J. Phys. Chem. **95**, 4948 (1991).
[10] Y. Miyamoto, A. Rubio, X. Blase, M. L. Cohen, and S. Louie, Phys. Rev. Lett. **74**, 2993 (1995).
[11] J. W. Mintmire and C. T. White, Phys. Rev. Lett. **81**, 2506 (1998).
[12] J. Wildöer, L. C. Venema, A. G. Rinzler, R. E. Smalley, and C. Dekker, Nature (London) **391**, 59 (1998).
[13] T. W. Odom, J.-L. Huang, P. Kim, and C. M. Lieber, Nature (London) **391**, 62 (1998).
[14] S. M. Sze, *Physics of Semiconductor Devices* (Wiley-Interscience, New York, 1981).
[15] While χ exhibits strong long-range oscillations at $2k_F$ for $T = 0$, these disappear at high temperature. At 300 K, oscillations in χ are insignificant for $f \lesssim 2 \times 10^{-3}$. [There are also oscillations in the *dielectric* susceptibility (in σ^{scr}), but at an atomic length scale.]
[16] Y. Imry and R. W. Landauer, Rev. Mod. Phys. **71**, S306 (1999).